Title
Developing a Bimolecular Affinity Purification Strategy to Isolate 26S Proteasome Holocomplexes for Complex-Centric Proteomic Analysis

Journal
Analytical Chemistry, 93(39)

ISSN
0003-2700

Authors
Yu, Clinton
Wang, Xiaorong
Li, Wenxue
et al.

Publication Date
2021-10-05

DOI
10.1021/acs.analchem.1c03551

Peer reviewed

Published in final edited form as:

Anal Chem. 2021 October 05; 93(39): 13407–13413. doi:10.1021/acs.analchem.1c03551.

Developing a Bimolecular Affinity Purification Strategy to Isolate 26S Proteasome Holocomplexes for Complex-centric Proteomic Analysis

Clinton Yu[1,#], **Xiaorong Wang**[1,#], **Wenxue Li**[2], **Yansheng Liu**[2], **Lan Huang**[1,*]

[1]Department of Physiology & Biophysics, University of California, Irvine, Irvine, CA 92694, USA

[2]Yale Cancer Biology Institute, Department of Pharmacology, Yale University, West Haven, CT 06516, USA

Abstract

The 26S proteasome is a mega-dalton protein complex responsible for the majority of intracellular degradation in eukaryotes. It is composed of two subcomplexes: the 20S core particle and 19S regulatory particle, which form compositionally and structurally heterogeneous proteasome complexes in cells. To fully characterize the 26S proteasome, it is necessary to understand its structural and functional diversities. Multiple mass spectrometric methodologies have been developed in recent years for the study of proteasome structural dynamics, in which biochemically isolated complexes are subjected for analysis. Due to the inherent heterogeneity of proteasome complexes, single-bait affinity purification typically results in a mixture of compositionally heterogeneous complexes regardless of the baits, making accurate assessment of complex-specific conformations and functions challenging. To facilitate complex-centric analysis, we have adopted a bimolecular affinity purification method utilizing a dual-bait cell line expressing a tagged 19S and a tagged 20S subunit to improve the homogeneity of the resulting 26S holocomplexes. To establish the method, four types of purifications were performed and the resulting samples were extensively examined by biochemical analysis and two label-free quantitative MS methods. Our results have demonstrated the effectiveness of this purification strategy to improve complex homogeneity for downstream biochemical and MS characterizations. This strategy will be valuable for facilitating detailed quantitative assessments of complex-specific molecular details under different conditions and can be directly adopted for studying other complexes.

Graphical Abstract

[*]Correspondence should be addressed to Dr. Lan Huang (lanhuang@uci.edu), Medical Science I, D233, Department of Physiology & Biophysics, University of California, Irvine, Irvine, CA 92697-4560, Phone: (949) 824-8548, Fax: (949) 824-8540.
[#]These authors contribute equally

COMPETING FINANCIAL INTERESTS

The authors declare no competing financial interests.

Supporting Information for Publication

- Additional experimental details, materials, and methods
- Supplemental figures and legends describing immunoblot results, DIA/DDA subunit quantitation, and quantitation correlation plots
- Supplemental tables detailing proteasome abundances in four types of purifications based on DIA and DDA quantitation

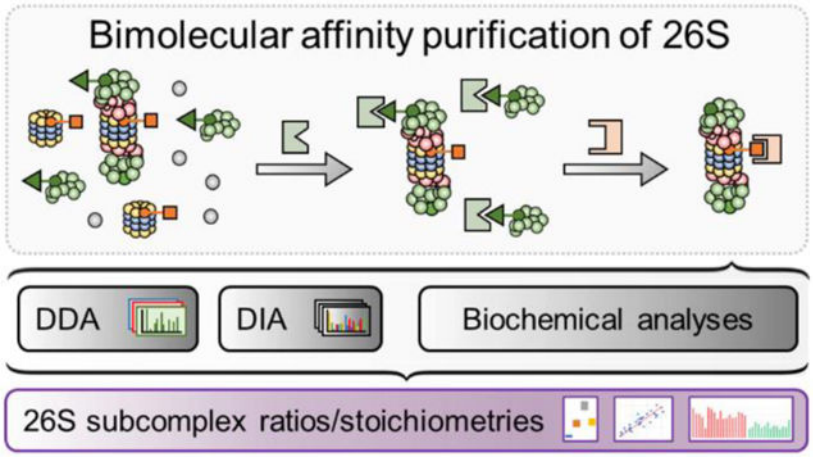

INTRODUCTION

The 26S proteasome is a ~2.5 MDa multisubunit protein complex responsible for the selective turnover of eukaryotic proteins in the ubiquitin/ATP-dependent protein degradation pathway [1]. The 26S holocomplex is composed of two subcomplexes: the 20S catalytic particle (CP) and 19S regulatory particle (RP). The 20S CP comprises seven α and seven β subunits arranged in an evolutionarily conserved cylindrical stack of four heptameric rings in the order αββα and harbors chymotrypsin-, trypsin-, and caspase-like enzymatic activity. In contrast, the 19S RP is composed of 19 subunits and is structurally dynamic compared to the 20S CP. The 19S RP can be further divided into two subcomplexes, the 19S base—made up of a hexamer ATPase ring (Rpt1-6) and four non-ATP subunits (Rpn1, 2, 10, and 13)—which directly interface the 20S CP, and the 19S lid—comprised of the remaining 9 non-ATPase subunits (Rpn3, 5–9, 11, 12, and 15/Sem1). Altogether, the 19S RP carries multiple functions to facilitate proteasomal degradation including substrate recognition, deubiquitylation, unfolding, and translocation as well as regulating the gate opening of 20S CP. In addition to 19S RP, the 20S CP can bind to alternative activator complexes such as the 11S (PA28)—heptameric rings composed of PA28γ or PA28α and PA28β—and PA200 [2,3]. These activators facilitate degradation through modulation of 20S proteasome structures, generating active 20S proteasomes by opening the 20S catalytic core and permitting ubiquitin/ATP-independent degradation of small proteins and peptides. Lastly, the compositional heterogeneity of proteasomes is further increased by the existence of hybrid proteasome complexes—20S proteasomes bound to two different types of activators (i.e. 19S-20S-11S [4], 19S-20S-PA200 [5]), which ultimately result in an array of pluriform complexes. Therefore, to define and quantify structural dynamics associated with specific proteasome complexes, it is a necessity to develop strategies to allow their effective isolation with desired compositional homogeneity.

Affinity purification coupled with mass spectrometry (AP-MS) has long since proven its effectiveness in isolating native protein complexes for proteomic characterization [6,7]. AP-MS strategies typically rely on either single-step or tandem-affinity purification of a single bait, with the former being advantageous in preserving protein-protein interactions

due to fewer sample preparation steps and the latter granting a higher purity and lower background but often losing weak interactions. To obtain functional proteasome complexes for biochemical and mass spectrometric analyses, we have previously developed a Histidine-Biotin (HB) tag-based affinity purification strategy to isolate functional 26S proteasome complexes from mammalian cells [8]. This strategy has been effective and allowed us to study their composition, post-translational modifications, and interactions [9,10]. In addition, we have successfully coupled the HB-based affinity purification strategy with cross-linking mass spectrometry (XL-MS) to elucidate architectures of the 26S proteasome and uncover the structural basis underlying its oxidative stress-mediated regulation [11,12]. The identified cross-links not only reveal protein interaction contacts, but also provide distance constraints for assisting computational modeling to elucidate protein structures. With quantitative XL-MS analyses, we have determined that the 26S proteasome undergoes conformational changes with one or more intermediate state(s) prior to its full disassembly in response to oxidative stress [13]. While successful, we have realized that complex heterogeneity complicates quantitative assessment of structural details at the peptide level. This is due to the fact that single bait-based affinity purification of proteasomes yields a mixture of 26S holocomplexes, and free 19S or 20S subcomplexes depending on whether 19S or 20S subunits are used as the bait. Cross-links detailing interactions with the 19S or 20S subunits could be attributed by holocomplexes, subcomplexes and/or both due to their presence in the purified mixture. To determine conformational dynamics of proteasome complexes, delineating structural changes based on cross-link quantitation requires proper normalization of protein abundance, however, this process has proven challenging for heterogeneous complexes [13]. Therefore, compositionally homogeneous complexes would be preferred to simplify such analysis. In addition to structural characterization, homogenous complexes would be beneficial to identify complex-specific proteomic profiles to characterize their distinct functions.

To improve homogeneity of purified protein complexes, bimolecular affinity purification (BAP) strategies have been previously developed, which utilize two separate protein baits in order to isolate complexes comprising both components [14–16]. In recent years, we have adopted this strategy and developed an *in vivo* cross-linking (X) assisted bimolecular tandem affinity purification (XBAP) method to stabilize and isolate dynamic ubiquitin receptor-bound proteasome subcomplexes [17]. The XBAP method derivatizes the HB tag into HF (His6-FLAG) and TB (TEV-Biotin) tags that are fused to the two selected baits respectively [17]. Here, we extended the XBAP strategy for separating 26S proteasome homocomplexes from other compositional forms by sequential purification with two protein baits from both the 19S and 20S subcomplexes. Mass spectrometric and biochemical analyses have demonstrated that this sequential approach results in nearly 90% removal of non-26S proteasome complexes relative to single-step purifications, significantly improving the homogeneity of purified 26S holocomplexes. Label-free quantitation of the resulting complexes based on both data-dependent acquisition (DDA) and data-independent acquisition (DIA) have allowed us to assess the relative abundances of the 19S and 20S complexes. This strategy will be valuable for facilitating detailed quantitative assessments of complex-specific molecular details under different conditions and can be directly adopted for studying other complexes.

EXPERIMENTAL PROCEDURES

Materials and Reagents

General chemicals for buffers and cell culture media were purchased from Fisher (Waltham, MA) or VWR (Radnor, PA). ImmunoPure streptavidin, HRP-conjugated antibody and Super Signal West Pico chemiluminescent substrate were from Pierce Biotechnology (Rockford, IL). Sequencing grade trypsin was purchased from Promega Corp. (Madison, WI), and anti-FLAG was from Sigma-Aldrich (St. Louis, MO).

Plasmids and Cloning

pQCXIH-Rpn11^{TB} and pQCXIP-β7^{HF} plasmid were constructed as described (Supplemental Methods).

Generation of 293$^{HF\text{-}β7/Rpn11\text{-}TB}$ Stable Cell Line

Briefly, a 293 GP2 cell line was co-transfected with pQCXIP-β7^{HF} or pQCXIH-Rpn11^{TB} as previously described [9,17]. Retroviruses were produced and released to the medium between 36 h to 96 h after transfection, and used to first transduce 293 cells with pQCXIP-β7^{HF} that were subsequently selected with puromycin, followed by transduction with pQCXIH-Rpn11^{TB} and selected with hygromycin to establish stable cell lines co-expressing Rpn11-TB and HF-β7, i.e. 293$^{HF\text{-}β7/Rpn11\text{-}TB}$.

Affinity Purification of Proteasomes

293$^{HF\text{-}β7/Rpn11\text{-}TB}$ cells were grown to confluence in DMEM medium containing 10% FBS and 1% Pen/strep. Before harvesting, cells were incubated with 0.025% formaldehyde for 10 min at 37 °C [11]. The cross-linked cells were then pelleted and washed with PBS, then lysed in native lysis buffer. 4 different proteasome purifications were performed on the clarified lysates: (1) incubation with streptavidin-agarose resin, (2) incubation with anti-FLAG M2 affinity gel and eluted with 3X FLAG peptide, (3) incubation with streptavidin-agarose resin and eluted by TEV cleavage, then further purified by binding to anti-FLAG affinity gel and eluted by 3X FLAG peptide, and finally (4) incubation with anti-FLAG affinity gel, eluted with 3x FLAG peptide, then further purified by binding to streptavidin-agarose resin. All purification fractions were analyzed by western blotting using α-Rpt6, α-β7, α-Flag and streptavidin-HRP. Purified proteins were reduced/alkylated and digested as described [18] (Supplemental Methods). The resulting peptide mixtures were then extracted and desalted prior to MS analyses. A minimum of 4 biological replicates were performed for each purification strategy.

LC MS/MS for Protein Identification and Quantitation with Data-Dependent Acquisition

The peptide digests were subjected to LC MS/MS analysis using an UltiMate 3000 RSLC system (Thermo Fisher Scientific) coupled in-line to an Orbitrap Fusion Lumos mass spectrometer (Thermo Fisher Scientific). MS/MS spectra were subjected to a developmental version of ProteinProspector (v.5.19.1) for database searching using Batch-Tag. MaxQuant was used to quantify the relative subcomplex composition in purified proteasomes. The average 19S/20S ratios for each type of purification were calculated based on the normalized

iBAQ abundances for 19S subunits and 20S subunits from each biological replicate, then averaged across all biological replicates for each purification. Details for data-dependent LC MS/MS analysis and database searching provided in Supplemental Methods.

LC MS/MS for Protein Identification and Quantitation with Data-Independent Acquisition

Peptide digests were subjected to LC MS/MS analysis using a Thermo EASY-nLC system (Thermo Fisher Scientific) coupled on-line to an Orbitrap Fusion Lumos mass spectrometer (Thermo Fisher Scientific). DIA-MS data analyses were performed using Spectronaut v.14 [19,20] using the "DirectDIA" pipeline (*i.e.,* an optimal spectral library-free pipeline [21]) Based on the purpose of subunit abundance estimation, no run-wise normalization was performed in Spectronaut. Details for data-independent LC MS/MS analysis and database searching provided in Supplemental Methods.

Proteasome Proteolytic Activity Assays

In-solution proteolytic activity assays for purified proteasomes were performed using fluorogenic peptide substrates SUC-LLVY-AMC, SUC-LLE-AMC, and SUC-ARR-AMC, as described previously [12] (Supplemental Methods). Three biological replicates were performed, and three technical replicates were analyzed for each biological replicate.

RESULTS and DISCUSSION

Developing a Bimolecular Affinity Purification Strategy to Isolate 26S Proteasome Holocomplexes

In order to improve the homogeneity of affinity purified 26S proteasome holocomplexes for detailed structural characterization, we have adopted the XBAP strategy [17] to eliminate the co-purification of free 19S and 20S complexes. The key element in this strategy is the generation of cells concurrently and stably expressing a tagged 19S subunit and a tagged 20S subunit to allow tandem affinity purification of 26S holocomplexes (Figure 1A). In this work, 19S subunit Rpn11 was fused to the TB tag and 20S subunit β7 was fused to the HF tag. These two subunits were selected due to their suitability for effectively purifying functional proteasome complexes [9,22]. Furthermore, it is noted that this strategy involves mild formaldehyde *in vivo* cross-linking to preserve the intactness of protein assemblies during purification steps. This has been shown to be effective for both dynamic proteasomes [13] and proteasome-ubiquitin receptor complexes [17], and can be widely applied for preservation of *in vivo* protein assemblies. Although native purifications were carried out in this work, the combination of HF and TB tags is versatile and permits BAP experiments under both native and denaturing conditions [9,11,17,23].

To evaluate XBAP-based analysis of the 26S proteasome, we performed four different purification experiments using stable $293^{\text{HF-}\beta7/\text{Rpn11-TB}}$ cells: two single-steps with a single bait and two two-steps with two baits affinity purifications, respectively (Figure 1B). The single-step purifications (Figure. 1B, path I) involve either a TB tag-based procedure through binding to streptavidin resin, or an HF-tag based isolation by binding to FLAG antibody resin. The two-step affinity purifications represent sequential purifications in the order of FLAG-Strep or Strep-FLAG (Figure. 1B, path II). It is expected that a mixture

of 26S proteasome holocomplexes plus free 19S or 20S subcomplexes would be obtained with a single bait, whereas two-bait purifications would result in 26S holocomplexes only (Figure 1B). Immunoblot analysis was carried out to examine the efficiencies of different purification strategies by probing a 19S subunit (Rpt6), a 20S subunit (β7), and the HF- and TB-tagged baits (Supplemental Figure 1). As shown, the abundance of the 19S subunit was reduced in the sequential Strep-FLAG purification compared to the single-step Strep-only purification, suggesting a decrease of co-purified free 19S complex during the Strep-FLAG purification (Supplemental Figure 1, left). Conversely, the efficiency of the FLAG-Strep sequential approach was similarly analyzed against the proteins isolated by FLAG-only purification (Supplemental Figure 1, right). In this comparison, the intensities of bands corresponding to the 20S subunit decreased dramatically compared to bands corresponding to the 19S subunit. Overall, the western blot analyses for both sequential purifications indicate an efficient removal of free subcomplex relative to their respective single-step purifications.

Label-free Quantitative Analysis of the 26S Proteasome via Data-Dependent Acquisition

To determine the homogeneity of proteasome purifications, we have performed LC MS/MS analysis of trypsin digests of the two-step purifications and their respective single-step preps (Figure 2). In this study, each purification type was repeated with at least 4 biological replicates which resulted in a total of 18 samples. Data-dependent acquisition (DDA)-based LC MS/MS runs allowed us to identify 32 subunits of the 26S proteasome complex in every purification as summarized in Supplemental Table S1.

To assess complex homogeneity, we first employed label-free quantitative analysis using MaxQuant [24]. In order to compare each purification strategy, iBAQ values for every proteasomal subunit were first obtained (Supplemental Table S2A) and normalized to the total proteasome content (Supplemental Table S2B). These values were then used to determine relative subunit composition in each sample (Supplemental Figure 2), as well as relative 19S and 20S abundances in each purification (Figure 3A). In general, we observed similar patterns for the relative abundances of individual subunits across all purifications, regardless of whether they were single or two-step. To estimate the relative subcomplex composition in purified proteasomes, we calculated average 19S/20S ratios for each type of purifications based on the normalized iBAQ abundances for 19S subunits and 20S subunits from each biological replicate. For FLAG-only purified proteasomes, the average quantitation ratio of 19S/20S was determined to be 0.29 (Figure 3C), suggesting an approximate 3:1 ratio of 20S to 19S abundance. To assess the similarities of protein measurements between replicate analyses, we employed a series of scatter plots to sample the correlation of 26S proteasome subunit abundances in every pair-wise combination of samples and we determined the average R^2 to be 0.90 (Supplemental Figure 3). For FLAG-Strep purified proteasomes, the average 19S/20S ratio was determined to be 0.61 (Figure 3C). Here, the average R^2 was calculated as 0.93 (Supplemental Figure 4). Comparing between the subunit abundances and 19S/20S ratios for FLAG-only and FLAG-Strep purifications indicates that the two-step purification reduced 20S content by about 21% and increased 19S content by ~61%, increasing the overall 19S content relative to 20S by about 105% (Figure 3E). Assuming all 20S in cell lysates were bound to FLAG resin during

the first step of the purification, our results suggest that approximately half of all 20S is not 19S-bound, either free or complexed with other activators, consistent with previous reports [25]. In comparison, the 19S/20S ratio of Strep-only purified proteasomes was found to be 1.15 and 0.72 in Strep-FLAG purifications (Figure 3C). Their average R^2 values were found to be 0.93 and 0.90, respectively (Supplemental Figures 5, 6). The difference in subunit abundances and 19S/20S ratios for Strep-only and Strep-FLAG purifications suggests that the two-step purification reduces the 19S content by ~19% and increases relative 20S content by ~28% compared to the single-step purification (Figure 3F). Therefore, these observations together indicate that the overall increase in 20S content relative to 19S is approximately 60%, corresponding to nearly a third of 19S present in lysate being removed during the 20S binding step of the Strep-FLAG purification. These results corroborated well with immunoblot analyses of purified proteasomes.

As described above, the 19S/20S ratios from FLAG-Strep (0.61) and Strep-FLAG (0.72) purification were close in value, yielding an average value of 0.66. The small difference observed here is most likely attributed to experimental variance between the two types of purifications. Assuming the two types of purifications (FLAG-Strep and Strep-FLAG) yield the same 26S holocomplexes, we estimated the removal of free 19S or 20S subcomplexes during the process based on the averaged 19S/20S ratios at each purification steps. As a result, ~93% free 20S was removed from the FLAG-Strep purification, whereas ~88% of free 19S was removed during the Strep-FLAG purification (Supplemental Table S4). These results indicate that the XBAP approach is an effective means of selectively purifying 26S holocomplexes by reducing sample heterogeneity that would otherwise hinder complex-specific quantitative analyses.

Label-free Quantitative Analysis of the 26S Proteasome via Data-Independent Acquisition (DIA)

In order to confirm the observations made from standard quantitative DDA analyses, we selected 17 samples that were analyzed by DDA described above for DIA-based LC MS/MS analysis. As a result, all 32 subunits considered for quantitative analysis in DDA were identified through DIA-MS and their protein abundances were determined (Supplemental Table S3A). Similarly, subunit abundances reported by DIA were normalized to total proteasome content (Supplemental Table S3B), then averaged across purification replicates and compared between single- and two-step purifications (Figure 3B; Supplemental Figure 7). As noted in the DDA, consistent patterns for individual subunit abundances were observed across all 4 purifications. Average R^2 statistics were determined similar to iBAQ values using pair-wise correlation plots (Supplemental Figures 8–11). The overall change in 19S and 20S subcomplexes were then used to determine the percent increase and decrease in relative abundances of intact 26S versus free 19S or 20S particles. 19S/20S abundance ratios for FLAG-only, FLAG-Strep, Strep-only, and Strep-FLAG purifications were determined via DIA to be 0.36, 0.63, 1.03, and 0.72 (Figure 3D, Supplemental Table S3B). The increase in relative abundance of 19S subunits when comparing FLAG-Strep to FLAG-only purifications was approximately 47%, whereas the relative abundance of 20S decreased by roughly ~18% (Figure 3E). When comparing Strep-FLAG to Strep-only purifications, the changes in 19S and 20S abundances were determined to be approximately −18% and +27%,

respectively. The overall increase in abundance of 20S relative to 19S was 55% (Figure 3F). Application of similar calculations to the DIA results has determined that ~92% of free 20S was removed with FLAG-Strep purification, whereas ~87% free 19S was removed during Strep-FLAG purification (Supplemental Table S4, bottom), correlating very well with DDA results as described above.

Biochemical Evaluation of Purified 26S Proteasomes

To examine the functionality of purified 26S proteasomes, we measured their proteolytic activities using fluorogenic peptide assays (Figure 4). Since both two-step purifications have yielded similar contents of 26S proteasomes, we selected FLAG-Strep purification for activity evaluation due to its experimental robustness. To fairly assess the differences, we measured proteasome activities in the forms that have been used for MS analyses. For FLAG-Strep purification, proteasomes bound on Strep beads were digested for quantitative analysis. Thus, on-bead activity assay was performed for FLAG-Strep preps and in-solution assay were carried out for the FLAG-only purification. Following normalization to proteasome levels determined by immunoblotting, the proteolytic activities of FLAG- and FLAG-Strep-purified proteasomes were determined to be relatively unchanged. These results suggest that the 26S abundance was preserved well during two-step purification, and that 19S-free 20S complexes have been effectively removed during the second step of the FLAG-Strep purification. Collectively, our results have demonstrated that the XBAP strategy is well suited for efficient purification of the human 26S holocomplexes with significantly improved complex homogeneity.

Characterization of Proteasome-Interacting Proteins (PIPs)

Apart from structural analysis, the developed purification strategy can be generalized to facilitate biochemical and MS analyses of purified protein complexes regarding their complex-specific functionality and proteome profiles including protein-protein interactions. In this case, subcomplex and holocomplex proclivities of proteasome-interacting proteins (PIPs) can be discerned from their quantitative profiles in each purification type. For example, label-free quantitation indicates that ubiquitin is present at similar abundances across FLAG-Strep, Strep-only, and Strep-FLAG but markedly decreased in FLAG-only purifications (Figure 5). This would be expected due to the role of ubiquitin in 26S-dependent proteasomal degradation and its recognition by the 19S RP. Proteasome-interacting proteins such as proteasome maturation protein (POMP) and proteasome assembly chaperones (PAC1 and PAC2) were detected abundantly in FLAG-only, but not in FLAG-Strep or other purifications (Figure 5). This suggests that these proteins are specific 20S proteasome interactors, and only bind to 19S-free 20S core particles. This is expected as PAC1 and PAC2 are directly involved with 20S α-ring assembly, and POMP is required for initiating subsequent β-ring formation [26]. On the other hand, while several proteasome activators (i.e. PA200, PA28α, PA28β, and PA28γ) were predominantly purified in FLAG-only, they were also detected in other three purifications (Figure 5). These observations coincide well with the fact that these proteasome activators bind to not only 19S-free 20S for non-ubiquitin-dependent degradation, but also to the 19S-bound 20S to form hybrid proteasome complexes. Other PIPs such as PAAF1, p27, and p28/Gankyrin were enriched in Strep-only purifications (Figure 5), corroborating with their functions in facilitating

assembly of the ATPase ring of the 19S RP [27]. These proteins remain associated throughout the assembly of the 19S and are released upon association with the 20S core. Finally, our results have shown that a known PIP, Ecm29, has a markedly higher abundance in Strep-only purifications compared to the other purified samples, indicating that Ecm29 has a preferred interaction with free 19S complex (Figure 5). This is not surprising as Ecm29 is important in regulating 26S proteasome disassembly in response to oxidative stress through enrichment on the 19S complex [12,18,28]. Collectively, these results have shown that the content of proteasome interactions is specific to the composition of proteasome complexes.

CONCLUSION

In this work, we have adopted a bimolecular affinity purification strategy to selectively purify 26S holocomplexes from cells containing compositionally diverse proteasome assemblies. Extensive quantitative MS analyses and biochemical assessments have demonstrated the effectiveness and robustness of the XBAP strategy established here to yield functional 26S complexes. The improved protein homogeneity will facilitate downstream complex-centric proteomic and biochemical investigations on dynamics, structure and function of 26S holocomplexes without interference of non-26S proteasome complexes. Importantly, this will simplify the protein normalization process during quantitative proteomic analysis, which is critical to XL-MS-based conformational studies of protein complexes. For QXL-MS experiments specifically, this enhancement translates to straightforward quantitative cross-link analysis. For example, future QXL-MS analysis of XBAP purified proteasomes would permit utilization of the entire cohort of cross-linking data, as cross-links would only originate from 26S proteasomes. In the absence of free 19S and 20S complexes, the observed changes in intra-subcomplex (19S or 20S) cross-link can be directly attributed to conformational dynamics within the entire 26S complex. In addition, comparing single- and two-bait purifications would permit profiling of complex-specific protein interactions and posttranslational modifications in the future. Moreover, this workflow can be employed to study the assembly/disassembly and subunit-dependent interactions of macromolecular protein complexes, as well as interactions between and within subcomplexes under different physiological conditions. In summary, the strategy described here represents a general and useful proteomic tool for isolating and studying specific protein complexes to reduce compositional heterogeneity for subsequent proteomic and biochemical inquiries.

Supplementary Material

Refer to Web version on PubMed Central for supplementary material.

ACKNOWLEDGMENT

We thank Drs. A.L. Burlingame, Robert Chalkley and Peter Baker for the developmental version of Protein Prospector. This work was supported by National Institutes of Health grants R01GM074830 and R01GM130144 to L.H., R01GM137031 as well as a Pilot Grant from Yale Cancer Center to Y.L..

ABBREVIATIONS

19S RP	19S Regulatory Particle
20S CP	20S Core Particle
AP-MS	Affinity Purification Mass Spectrometry
BAP	Bimolecular Affinity Purification
DDA	Data-Dependent Acquisition
DIA	Data-Independent Acquisition
iBAQ	intensity-Based Absolute Quantification
PPI	Protein-protein interaction
PTM	Post-translational modification
XBAP	cross (X)-linking assisted Bimolecular tandem Affinity Purification
XL-MS	cross (X)-Linking Mass Spectrometry

REFERENCES:

(1). Voges D; Zwickl P; Baumeister W The 26S proteasome: a molecular machine designed for controlled proteolysis. Annu Rev Biochem. 1999, 68, 1015–1068. [PubMed: 10872471]

(2). Finley D Recognition and processing of ubiquitin-protein conjugates by the proteasome Annu Rev Biochem 2009, 78, 477–513. [PubMed: 19489727]

(3). Stadtmueller BM; Hill CP Proteasome activators Mol Cell 2011, 41, 8–19. [PubMed: 21211719]

(4). Hendil KB; Khan S; Tanaka K Simultaneous binding of PA28 and PA700 activators to 20 S proteasomes Biochem J 1998, 332 (Pt 3), 749–754. [PubMed: 9620878]

(5). Blickwedehl J; Agarwal M; Seong C; Pandita RK; Melendy T; Sung P; Pandita TK; Bangia N Role for proteasome activator PA200 and postglutamyl proteasome activity in genomic stability Proc Natl Acad Sci U S A 2008, 105, 16165–16170. [PubMed: 18845680]

(6). Snider J; Kotlyar M; Saraon P; Yao Z; Jurisica I; Stagljar I Fundamentals of protein interaction network mapping Mol Syst Biol 2015, 11, 848. [PubMed: 26681426]

(7). Richards AL; Eckhardt M; Krogan NJ Mass spectrometry-based protein-protein interaction networks for the study of human diseases Mol Syst Biol 2021, 17, e8792. [PubMed: 33434350]

(8). Lu P; Vogel C; Wang R; Yao X; Marcotte EM Absolute protein expression profiling estimates the relative contributions of transcriptional and translational regulation Nature biotechnology 2007, 25, 117–124.

(9). Wang X; Chen CF; Baker PR; Chen PL; Kaiser P; Huang L Mass spectrometric characterization of the affinity-purified human 26S proteasome complex Biochemistry 2007, 46, 3553–3565. [PubMed: 17323924]

(10). Wang X; Huang L Identifying dynamic interactors of protein complexes by quantitative mass spectrometry Mol Cell Proteomics 2008, 7, 46–57. [PubMed: 17934176]

(11). Wang X; Cimermancic P; Yu C; Schweitzer A; Chopra N; Engel JL; Greenberg C; Huszagh AS; Beck F; Sakata E; Yang Y; Novitsky EJ; Leitner A; Nanni P; Kahraman A; Guo X; Dixon JE; Rychnovsky SD; Aebersold R; Baumeister W, et al. Molecular Details Underlying Dynamic Structures and Regulation of the Human 26S Proteasome Mol Cell Proteomics 2017, 16, 840–854. [PubMed: 28292943]

(12). Wang X; Chemmama IE; Yu C; Huszagh A; Xu Y; Viner R; Block SA; Cimermancic P; Rychnovsky SD; Ye Y; Sali A; Huang L The proteasome-interacting Ecm29 protein disassembles

the 26S proteasome in response to oxidative stress The Journal of biological chemistry 2017, 292, 16310–16320. [PubMed: 28821611]

(13). Yu C; Wang X; Huszagh AS; Viner R; Novitsky E; Rychnovsky SD; Huang L Probing H2O2-mediated Structural Dynamics of the Human 26S Proteasome Using Quantitative Cross-linking Mass Spectrometry (QXL-MS) Mol Cell Proteomics 2019, 18, 954–967. [PubMed: 30723094]

(14). Maine GN; Gluck N; Zaidi IW; Burstein E Bimolecular affinity purification (BAP): tandem affinity purification using two protein baits Cold Spring Harb Protoc 2009, 2009, pdb prot5318. [PubMed: 20150057]

(15). Starokadomskyy P; Burstein E Bimolecular affinity purification: a variation of TAP with multiple applications Methods Mol Biol 2014, 1177, 193–209. [PubMed: 24943324]

(16). Liu X; Zhang Y; Wen Z; Hao Y; Banks CAS; Lange JJ; Slaughter BD; Unruh JR; Florens L; Abmayr SM; Workman JL; Washburn MP Driving integrative structural modeling with serial capture affinity purification Proc Natl Acad Sci U S A 2020, 117, 31861–31870. [PubMed: 33257578]

(17). Yu C; Yang Y; Wang X; Guan S; Fang L; Liu F; Walters KJ; Kaiser P; Huang L Characterization of Dynamic UbR-Proteasome Subcomplexes by In vivo Cross-linking (X) Assisted Bimolecular Tandem Affinity Purification (XBAP) and Label-free Quantitation Mol Cell Proteomics 2016, 15, 2279–2292. [PubMed: 27114451]

(18). Zhu Y; Wang WL; Yu D; Ouyang Q; Lu Y; Mao Y Structural mechanism for nucleotide-driven remodeling of the AAA-ATPase unfoldase in the activated human 26S proteasome Nature communications 2018, 9, 1360.

(19). Bruderer R; Bernhardt OM; Gandhi T; Miladinovic SM; Cheng LY; Messner S; Ehrenberger T; Zanotelli V; Butscheid Y; Escher C; Vitek O; Rinner O; Reiter L Extending the limits of quantitative proteome profiling with data-independent acquisition and application to acetaminophen-treated three-dimensional liver microtissues Mol Cell Proteomics 2015, 14, 1400–1410. [PubMed: 25724911]

(20). Bruderer R; Bernhardt OM; Gandhi T; Xuan Y; Sondermann J; Schmidt M; Gomez-Varela D; Reiter L Optimization of Experimental Parameters in Data-Independent Mass Spectrometry Significantly Increases Depth and Reproducibility of Results Mol Cell Proteomics 2017, 16, 2296–2309. [PubMed: 29070702]

(21). Tsou CC; Avtonomov D; Larsen B; Tucholska M; Choi H; Gingras AC; Nesvizhskii AI DIA-Umpire: comprehensive computational framework for data-independent acquisition proteomics Nat Methods 2015, 12, 258–264, 257 p following 264. [PubMed: 25599550]

(22). Lee MJ; Lee BH; Hanna J; King RW; Finley D Trimming of ubiquitin chains by proteasome-associated deubiquitinating enzymes Mol Cell Proteomics 2011, 10, R110 003871.

(23). Guerrero C; Tagwerker C; Kaiser P; Huang L An integrated mass spectrometry-based proteomic approach: quantitative analysis of tandem affinity-purified in vivo cross-linked protein complexes (QTAX) to decipher the 26 S proteasome-interacting network Mol Cell Proteomics 2006, 5, 366–378. [PubMed: 16284124]

(24). Cox J; Mann M MaxQuant enables high peptide identification rates, individualized p.p.b.-range mass accuracies and proteome-wide protein quantification Nat Biotechnol 2008, 26, 1367–1372. [PubMed: 19029910]

(25). Ben-Nissan G; Sharon M Regulating the 20S proteasome ubiquitin-independent degradation pathway Biomolecules 2014, 4, 862–884. [PubMed: 25250704]

(26). Tanaka K The proteasome: overview of structure and functions Proc Jpn Acad Ser B Phys Biol Sci 2009, 85, 12–36.

(27). Besche HC; Peth A; Goldberg AL Getting to first base in proteasome assembly Cell 2009, 138, 25–28. [PubMed: 19596233]

(28). Wang X; Yen J; Kaiser P; Huang L Regulation of the 26S proteasome complex during oxidative stress Sci Signal 2010, 3, ra88. [PubMed: 21139140]

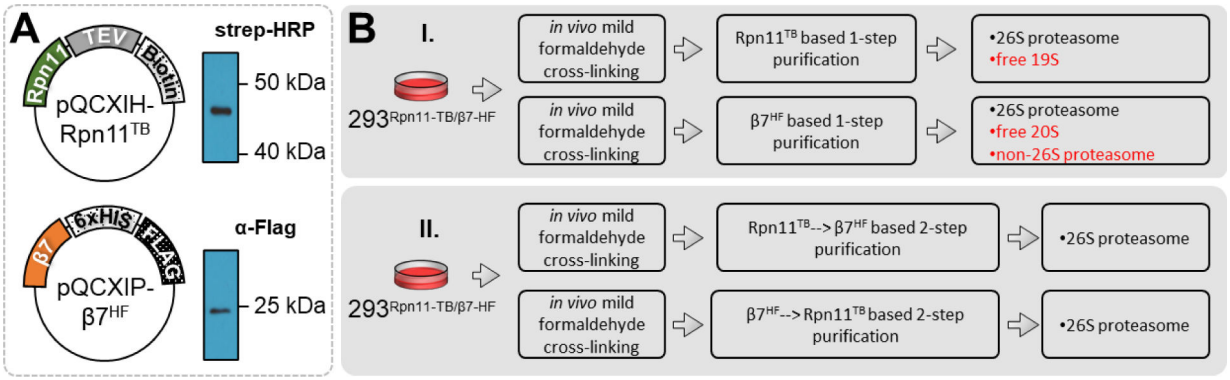

Figure 1. Bimolecular purification strategy.

(A) Constructs of pQCXIH-Rpn11^{TB} and pQCXIP-β7^{HF} and protein expression of Rpn11^{TB} and β7^{HF}, respectively. **(B)** Human proteasome complexes were isolated from stable cell lines 293$^{Rpn11\text{-}TB/β7\text{-}HF}$ using single-step (Path I) or two-step (Path II) purification strategies.

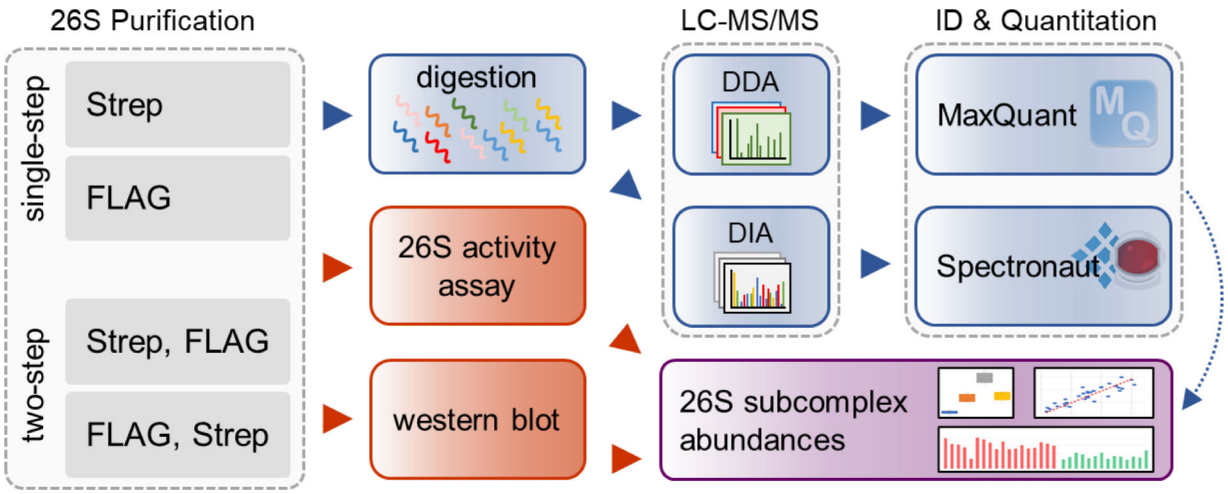

Figure 2. Workflow for proteasome sample preparation and analyses.

Purified proteasomes were digested and analyzed by LC MS/MS using data-dependent and data-independent acquisition strategies, respectively, and directly assessed by proteolytic activity assays and western blot analysis.

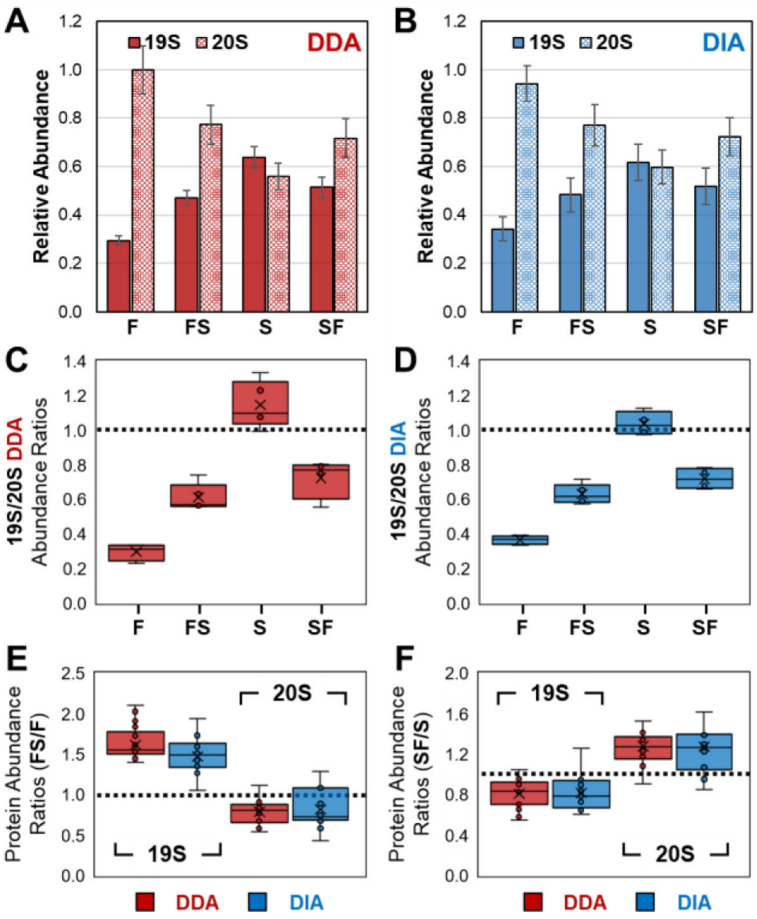

Figure 3. Quantitation of purified 26S proteasome subcomplexes.

(A-B) Abundances of 19S and 20S subcomplexes in each purification strategy as determined by DDA- and DIA-based quantitation, respectively. Subcomplex abundance was calculated as the average of all corresponding subunits, across all biological replicates. **(C-D)** Abundance ratios of 19S to 20S subcomplexes for each purification were calculated based on DDA and DIA quantitation, respectively. **(E-F)** Abundance changes of 19S and 20S subcomplexes when comparing between FLAG-strep and FLAG-only purifications, or Strep-FLAG and Strep-only purifications, respectively. In all graphs, red-shaded boxes represent values determined through data-dependent analyses; blue boxes represent values acquired through data-independent analyses. Note: F: FLAG-only; FS: FLAG-Strep; S:Strep; SF: Strep-FLAG.

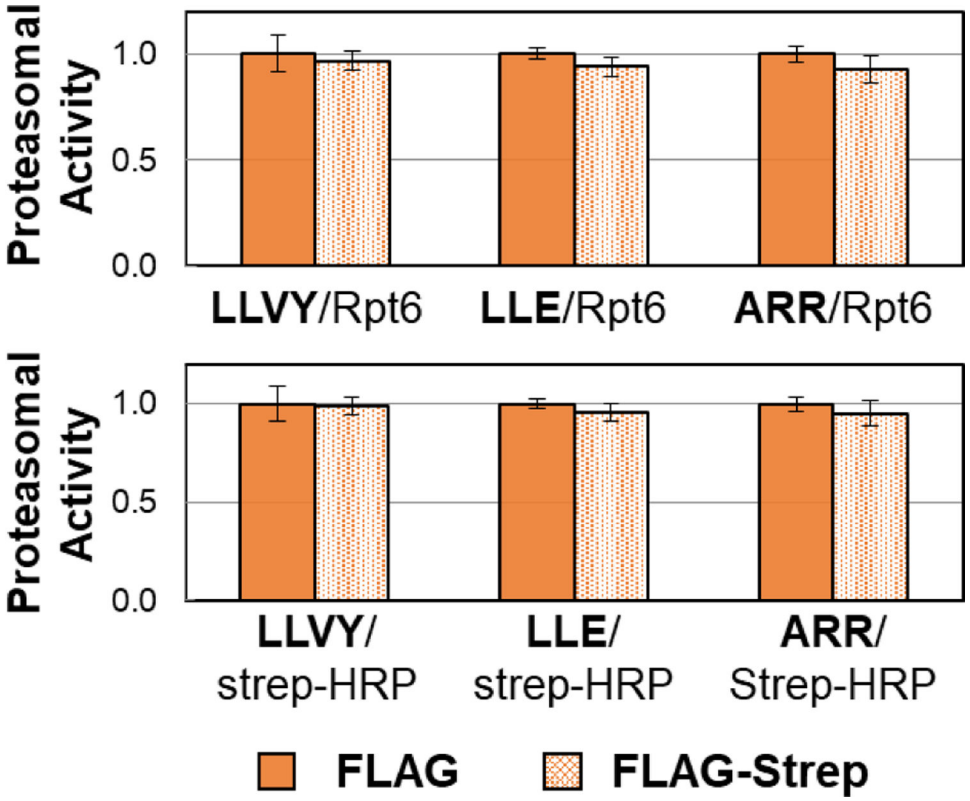

Figure 4. Proteasomal activity assays.

Activity of proteasomes from FLAG-only and FLAG-Strep purifications were measured using fluorogenic peptide substrates SUC-LLVY-AMC, SUC-LLE-AMC, and SUC-ARR-AMC. The proteasome activity was normalized by the band intensity of α-Rpt6 (top) and streptavidin-HRP (bottom). Results shown are the average of triplicate measurements.

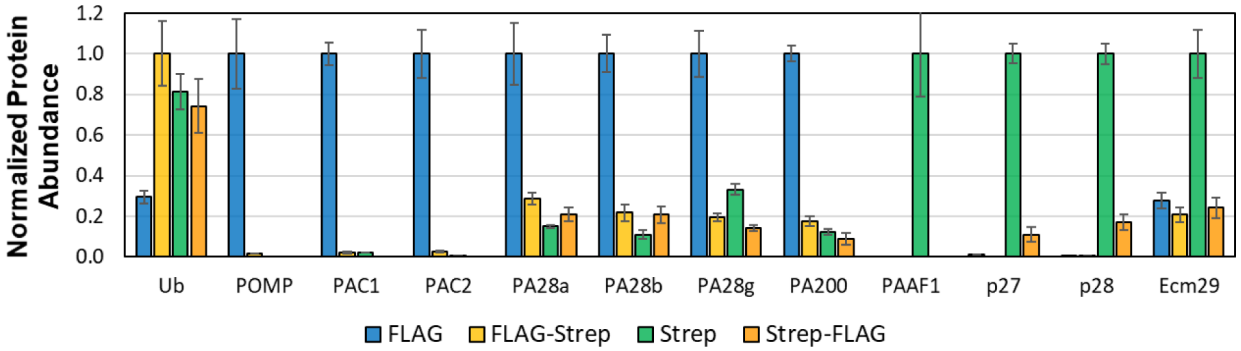

Figure 5.

Relative abundances of selected proteasome-interacting proteins (PIPs) across single- and two-step purifications. Abundances for each protein were normalized to the purification type with highest intensity.